GLOBAL MORPHOLOGIC MAP OF TESSERAE ON VENUS. R. S. Albach[1] and J. L. Whitten[1], [1]Department of Earth and Environmental Sciences, Tulane University, New Orleans, LA (ralbach@tulane.edu).

Introduction: Tesserae are regions of high radar backscatter and tectonic deformation that cover ~8% of the surface of Venus [1]. Despite being the oldest units on Venus [1], many open questions about tesserae remain like their composition, surface evolution, and formation mechanism. Proposed formation mechanisms include upwelling or downwelling of the mantle [2, 3]. Tesserae material has been variously proposed to be basaltic or felsic [4, 5]. Comprehensive global studies aimed at determining the composition and formation mechanism(s) of tesserae are limited by available global datasets of the surface of Venus from the Magellan mission (SAR, emissivity, topography), VIRTIS on Venus Express, and low-resolution radar data from Arecibo.

Previous global mapping efforts do not divide all tesserae by morphology [1, 6], although many regional maps do have comprehensive morphologic division [7–12]. Here we present the preliminary results of ongoing global morphologic mapping of Venusian tesserae. A global morphologic map will facilitate comparisons between existing regional observations of tesserae [e.g., 13] and variations in surface morphology.

Methodology: The Magellan SAR left look global mosaic (spatial resolution of 75 meters per pixel) was used to map tesserae based on morphology. Initial mapping was completed in ArcGIS Pro at a scale of 1:750,000 and covered Alpha Regio, Phoebe Regio, Manatum Tessera, Ovda Regio, Aphrodite Terra, and Thetis Regio. Individual tesserae are divided into texturally-distinct regions. "Texturally distinct" describes differences in the spacing, the shape, and the orientation of the tectonic features such as graben, fractures, and ridges that compose tesserae. Each texturally distinct region was grouped into classes (e.g., A, B, C) based on the similarity of their surface morphologies.

The Magellan SAR base map is dynamically-stretched using the screen area for radar-bright tesserae. Dynamic stretching prevents high average backscatter coefficient values from obscuring textural variations in regions such as Thetis Regio.

Preliminary Results: The current morphologic map includes fifteen textural categories and covers most low-latitude tesserae (Fig. 1). The textures with the largest mapped areas are A, C, D, and K, with areas of 1.79×10^6 km^2, 1.62×10^6 km^2, 1.35×10^6 km^2, and 1.13×10^6 km^2, respectively (Fig. 2). In all, the current textural classes range in area from 1.79×10^6 km^2 to 3.47×10^4 km^2. Texture A consists of closely spaced intersecting ridges and troughs and occurs on the

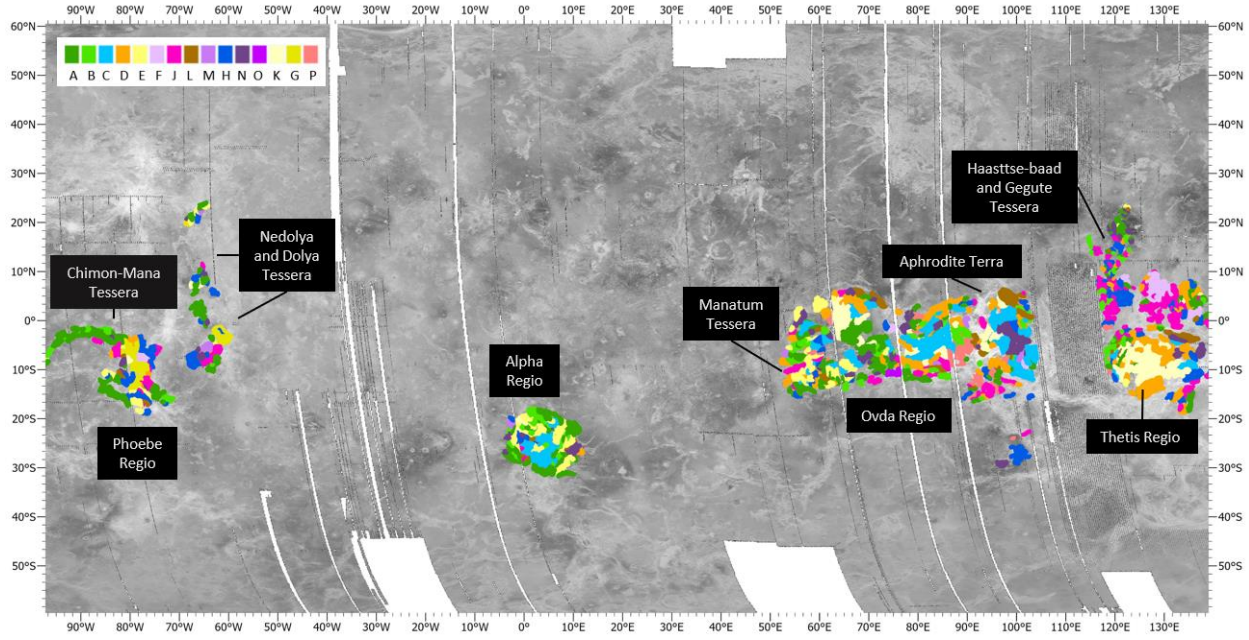

Figure 1: Current extent of tesserae textural classification across Venus. Texture names (A, B, C, etc.) correspond to those in Figs. 2 and 3. The base map is Magellan left look SAR data (75 m/pixel). Like colors (the greens, purples, yellows, and blues) indicate textural similarities with other classes of the same color.

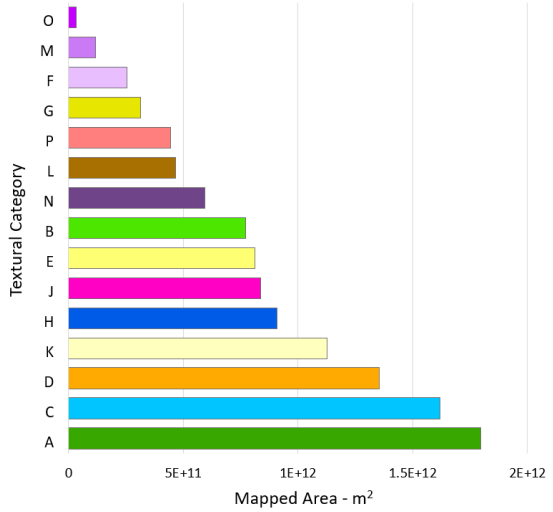

Figure 2: Textural categories organized by mapped area (m^2).

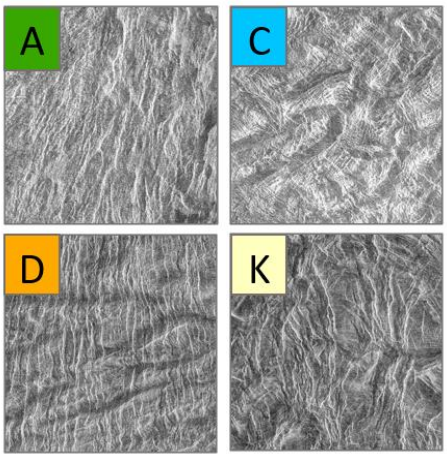

Figure 3: Example textures from the four most areally extensive categories. Swatches are of the Magellan Left Look SAR data (75 m/pixel) and are ~10,000 km^2.

perimeter of Alpha Regio, Chimon-mana Tessera, and Dolya Tessera but on both the interior and perimeter of Manatum Tessera (Fig. 1, dark green). Other extensive textures include C, which features arcuate ridges and troughs, and D, which has fractures orthogonal to broad grabens.

Initial mapping reveals that some tesserae have predominant textures, such as texture K in Thetis Regio, while other tesserae show a patchwork of smaller-extent textures (e.g., Manatum Tessera, Gegute Tessera). Texture G has only been identified in Chimon-mana Tessera, Nedolya Tessera and Dolya Tessera, while other textures, such as A and J, were identified in all tesserae.

Discussion and Conclusion: Some textural categories identified in this study coincide with those used in other morphologic maps of Venusian tesserae [1, 8, 9]. For example, texture C corresponds with basin-and-dome terrain, texture G with "star" terrain, and texture P with "lava flow" terrain [9].

Some of the classes identified in initial mapping are texturally similar. Textures O, M, F, and N all have intersecting tectonic features arranged at acute to orthogonal angles to one another. Textures O, M, and F have the lowest mapped areal extents of $3.47x10^4$ km^2, $1.18x10^5$ km^2, and $2.53x10^5$ km^2, respectively (Fig. 2). In the map, like textural classes often occur in close or immediate proximity. Textural classes such as O, M, F, and N may be combined in the final map due to their small areal extent, proximity, and similarity in texture.

Texturally similar classes may differ due to post-emplacement modification, such as embayment by flood volcanism or mantling by crater ejecta [1, 9, 14]. Comparison of the backscatter coefficients with mapped textures could reveal areas mantled by ejecta or otherwise modified. Mantled tesserae backscatter coefficients will differ from those of the same texture [14].

Continued mapping will result in a global morphologic map of major tesserae that follows the methodology described here. Textural categories may be added or combined according to the textures of the yet unmapped tesserae. A global morphologic map of Venusian tesserae will show global trends that may reveal clues to the timing and mechanism(s) of tesserae formation. For example, tesserae with areally extensive textural units (like C in Ovda Regio and K in Thetis Regio) indicate blocks of tesserae with similar deformation histories. Further study of the relationship between the morphology and the radar properties of tesserae globally allows investigation into how the diversity of tesserae on Venus may reveal one or a variety of formation and modification mechanisms, compositions, and ages, all of which are still debated.

References: [1] Ivanov M. & Head J. (1996) *JGR, 101*, 14861-14908. [2] Phillips R. et al. (1991) *Science*, 252, 651-658. [3] Bindschadler et al. (1992) *JGR*, 97, 13495-13532. [4] Ivanov M. (2001) *Solar System Research*, 35, 1-17. [5] Mueller N. et al. (2008) *JGR*, 113, E00B17. [6] Senske D. A. et al. (1994) LPSC XXV, 1245-1246 (abs.). [7] Gilmore M. & Head J. (2018) *Planetary and Space Science, 154*, 5–20. [8] Bindschadler D. et al. (1992) *JGR, 97*, 13563–13577. [9] Hansen V. & Willis J. (1996) *Icarus, 123*, 296–312. [10] Bindschadler D. & Head J. (1991) *JGR, 96*, 5889–5907. [11] Bruegge R. & Head J. (1989) *GRL, 16*, 699-702. [12] Bender K. et al. (2000) *Icarus, 148*, 153-159. [13] Brossier J. & Gilmore M. (2020) LPSC LI, 1026 (abs.). [14] Campbell B. et al. (2015) *Icarus, 250*, 123-130.